when some of the f_j may be negative), a situation which appears rarely, if ever, to occur in practice, the distributions (3.3) and (3.5) reduce to the conditional distribution of φ when only the five magnitudes (1.1) of the first neighborhood are given, so that nothing is gained by going to the second neighborhood of φ. Since the same phenomenon has already been observed for quartets (Hauptman, 1976), it is beginning to appear that the condition $\sigma_3 \neq 0$ may be a necessary one for a solution of the phase problem to exist; but a final resolution of this question will have to await further developments. (There is some evidence which suggests that the more stringent requirement $(3\sigma_3^2-\sigma_2\sigma_4)/\sigma_2^3>0$ may in fact be necessary.) In the X-ray diffraction case there is no problem since then every f_j is positive, and σ_3 is therefore also positive. Furthermore, in the applications to neutron diffraction the condition $\sigma_3^2/\sigma_2^3=0$ appears rarely, if ever, to be fulfilled, so that the results derived here are almost sure to be useful for neutron diffraction as well.

Finally, the initial applications of quintets have been made (Fortier, Fronckowiak & Hauptman, 1977; Fronckowiak, Fortier, De Titta & Hauptman, 1977). These show that quintets will be at least as important in the applications as quartets or triples, and strongly suggest that the use of all available invariants and seminvariants will be more useful still.

This research was supported in part by Grant No. MPS73-04992 from the National Science Foundation, DHEW Grant Nos. HL15378 and RR05716, and Ministère de l'Education, Gouvernement du Québec.

References

FORTIER, S., FRONCKOWIAK, M. & HAUPTMAN, H. (1977). ACA Meeting February 21–25, 1977, Asilomar, Ca., Abstract KM 1.

FORTIER, S. & HAUPTMAN, H. (1977). *Acta Cryst.* A**33**, 572–575.

FRONCKOWIAK, M., FORTIER, S., DE TITTA, G. & HAUPTMAN, H. (1977). ACA Meeting February 21–25, 1977, Asilomar, Ca., Abstract KM 3.

HAUPTMAN, H. (1975). *Acta Cryst.* A**31**, 680–687.

HAUPTMAN, H. (1976). *Acta Cryst.* A**32**, 877–882.

HAUPTMAN, H. (1977). *Acta Cryst.* A**33**, 568–571.

Acta Cryst. (1977). A**33**, 580–584

Experimental Charge Density Distribution in Potassium Azide by Diffraction Methods

BY EDWIN D. STEVENS

Department of Chemistry, State University of New York at Buffalo, Buffalo, New York 14214, *USA*

(*Received* 5 *October* 1976; *accepted* 20 *December* 1976)

The electron density distribution of potassium azide is determined from high-resolution X-ray intensity measurements. The calculated distributions of errors in the experimental densities are included. Refinement of high-order X-ray data yields parameters in good agreement with neutron diffraction results. The inclusion of high-order data in calculating the deformation density is found to be necessary to obtain a quantitative distribution. Densities calculated with only low-order data are qualitatively similar but lack detail in the shape as well as in the height of the bonding features.

Introduction

In recent years, methods have been developed for direct experimental determination of the electron distribution in solids using accurate X-ray and neutron diffraction measurements (Coppens, 1975). An obvious objective is the comparison of experimental results with theoretical calculations of the electron density distribution. For several reasons, most previous comparisons have been unsatisfactory (Coppens & Stevens, 1976). The electron density distribution has been found to be a very sensitive function of the quality of the wavefunction, but because of computational limitations, the sophisticated calculations necessary are at present available only for very small molecules. On the other hand, small-molecule systems are experimentally difficult since they are often gases or liquids at room temperature.

Experimental studies of the electron density distribution in the azide ion have been undertaken for comparison with *ab initio* molecular-orbital calculations (Stevens, Rys & Coppens, 1977*a*,*b*). The present study of potassium azide complements a recent experimental study of the azide ion in the structure of NaN_3 (Stevens & Hope, 1977). The studies of the azide ion in two different crystal forms provide additional information on the effects of the crystal field and thermal smearing.

A detailed analysis of the experimental error distribution has been included so that the significance of features in the experimental density maps can be assessed.

Experimental methods

X-ray data collection and processing

A small single crystal with dimensions 0·22 × 0·20 ×

0·10 mm was obtained by slow evaporation of an aqueous solution. The crystal was mounted in an arbitrary orientation on a Picker FACS-I automatic diffractometer and X-ray data collected using Nb-filtered Mo $K\alpha$ radiation. Crystallographic information is summarized in Table 1. The full 2θ step-scan profile on each reflection was recorded on magnetic tape and analyzed to give the integrated intensity and its standard deviation (Blessing, Coppens & Becker, 1974). In all 3463 reflections were collected in the range $0{\cdot}0 < \sin\theta/\lambda < 1{\cdot}2$ Å^{-1}.* This corresponds to approximately six symmetry-related forms of each independent reflection. Three standard reflections measured after every 50 reflections showed no significant change in intensity. Absorption corrections were calculated by Gaussian numerical integration (Coppens, Leiserowitz & Rabinovich, 1965). Averaging symmetry-related reflections gave 511 unique reflections, of which 366 were at $\sin\theta/\lambda > 0{\cdot}75$ Å^{-1}. The internal agreement index $R(F^2)$ between symmetry-related reflections was 2·2%.

Table 1. *Crystallographic data for potassium azide*

Tetragonal	Space group: *I*4/*mcm*
$a = 6{\cdot}1188\,(6)$ Å	$M = 81{\cdot}12$
$c = 7{\cdot}1015\,(10)$	$U = 265{\cdot}9$ Å^3
	$Z = 4$
$D_x = 2{\cdot}026$ g cm^{-3}	μ(Mo $K\alpha$) = 16·65 cm^{-1}

* A list of structure factors has been deposited with the British Library Lending Division as Supplementary Publication No. SUP 32413 (4 pp.). Copies may be obtained through The Executive Secretary, International Union of Crystallography, 13 White Friars, Chester CH1 1NZ, England.

Least-squares refinement

The quantity $\Sigma w(F_o - k|F_c|)^2$ with $w = 1/\sigma^2$ was minimized by full-matrix least-squares refinement including adjustment of an isotropic extinction parameter (Becker & Coppens, 1975). The best fit to the observed intensities was obtained from a Type I extinction model with a Lorentzian mosaic distribution. Standard deviations were estimated using $\sigma^2(I) = C^2I^2 + \sigma^2_{\text{count}}$ with $C = 0{\cdot}015$. Atomic scattering factors calculated from Hartree–Fock atomic wavefunctions (HF) were taken from Doyle & Turner (1968). In some refinements (Table 2), scattering factors for nitrogen calculated from a best spherical atom fit (BSAF) to a molecular wavefunction of the azide ion were used (Stevens & Hope, 1977). Anomalous dispersion values for K and N were taken from Cromer & Liberman (1970).

To reduce the bias in refined parameters from the aspherical valence electron distribution, high-order refinements were made using only reflections with $\sin\theta/\lambda > 0{\cdot}75$ Å^{-1}. Results of various refinements are listed in Table 2. Standard deviations of the refined parameters were obtained from the full least-squares variance–covariance matrix.

Electron density maps

The effects of chemical bonding are best revealed in a deformation density map. The deformation density $\Delta\varrho$ is the difference between the observed density and the density calculated from a superposition of spherical, neutral Hartree–Fock atoms,

$$\Delta\varrho = \frac{\varrho_{\text{obs}}}{k} - \varrho_{\text{calc}}.$$

Table 2. *Results of various refinements*

		HF	HF	BSAF	BSAF	Neutron*
$\sin\theta/\lambda$ range (Å^{-1})		0–0·75	0·75–1·25	0–0·75	0·75–1·25	0–0·83
k		1·981 (7)	1·952 (10)	1·959 (5)	1·965 (10)	
K	U_{11} (Å$^2 \times 10^4$)	235 (2)	231 (1)	232 (2)	232 (1)	214 (5)
	U_{33}	214 (2)	211 (1)	209 (2)	212 (1)	179 (6)
N(2)	U_{11} (Å$^2 \times 10^4$)	181 (5)	167 (1)	170 (3)	167 (2)	168 (4)
	U_{33}	213 (9)	240 (3)	205 (6)	240 (3)	231 (2)
	U_{12}	44 (7)	12 (4)	44 (4)	12 (4)	12 (2)
N(1)	x ($\times 10^5$)	13611 (15)	13626 (10)	13594 (9)	13628 (10)	13576 (6)
	U_{11} (Å$^2 \times 10^4$)	220 (4)	209 (2)	215 (3)	211 (2)	213 (4)
	U_{33}	380 (8)	388 (4)	393 (5)	392 (4)	383 (3)
	U_{12}	−21 (5)	−30 (2)	−20 (4)	−29 (2)	−32 (2)
g (extinction)† ($\times 10^6$)		5·7 (5)	[5·7]	4·7 (3)	[4·7]	
R (%)		1·2	6·6	0·7	4·3	2·0
R_w (%)		1·8	2·2	0·8	2·1	2·2
GOF‡		4·69	1·32	2·48	1·26	
N_{obs}		145	366	145	366	166
N_v		11	10	11	10	

* Choi & Prince (1976).
† Values in brackets not refined.
‡ 'Goodness of fit' = $[\Sigma w(F_o - k|F_c|)^2/(N_{\text{obs}} - N_v)]^{1/2}$.

The designations $X-N$ and $X-X$ refer to maps in which ϱ_{calc} has been obtained from neutron or high-order X-ray positional and thermal parameters, respectively. Neutron parameters were taken from the results of Choi & Prince (1976).

All maps were calculated using the full X-ray data set, corrected for extinction and anomalous dispersion. The scale factor was obtained by a cycle of refinement on k with fixed neutron or high-angle X-ray atomic parameters.

Error maps

Calculation of the error distribution in deformation density maps has recently been described by Rees (1976). Neglecting correlation between ϱ_{obs}, ϱ_{calc}, and k, the variance in deformation density is given by

$$\sigma^2(\Delta\varrho)=\sigma^2(\varrho_{obs})/k^2+\sigma^2(\varrho_{calc})+\left[\frac{\sigma^2(k)}{k^2}\right]\left[\frac{\varrho_{obs}^2}{k^2}\right].$$

The contributions to $\sigma(\Delta\varrho)$ have been evaluated and plotted in a manner similar to Rees (1976) with the exception that the correlations between positional parameters, thermal parameters and the scale factor have been included explicitly. Contributions from $\sigma(\varrho_{calc})$ and $\sigma(k)$ have been calculated analytically (Stevens & Coppens, 1976) and thus these contributions of the error densities are not series terminated.

Discussion

Parameters refined from conventional (low-order) X-ray data are biased by the attempts of the least-squares procedure to fit the aspherical valence density with a spherical-atom model. The bias can be reduced by refinement using only high-order data (Stevens & Hope, 1975). For KN_3, high-order refinement gives higher R values, owing to the lower statistical accuracy of the many weak reflections, but a lower goodness-of-fit value and good agreement with the neutron diffraction results for the nitrogen parameters (Table 2).

The differences between the nitrogen low-order parameters and the high-order or neutron parameters found in KN_3 are similar to those found for NaN_3 (Stevens & Hope, 1977). In the low-order results, the apparent mean square amplitude of vibration of the center nitrogen along the bond (0·0225 $Å^{-2}$) is larger than the vibration of the end nitrogen (0·0199 $Å^{-2}$), and reflects the attempt of the least-squares refinement to fit the N–N bonding density.

Although the BSAF scattering factors were calculated from a limited-basis-set wavefunction (Stevens, 1973), refinement with nitrogen BSAF scattering fac-

Table 3. *Rigid-body thermal parameters* ($\times 10^4$) *for* N_3^- *in* KN_3

$U_{11}=U_{22}$, $U_{13}=U_{23}=0$, $L_{11}=L_{22}=-L_{12}$, $L_{13}=L_{23}$

	X-ray (high-order)	Neutron (Choi & Prince, 1976)
U_{11}	168 (1) Å^2	168 (4) Å^2
U_{33}	240 (1)	230 (4)
U_{12}	14 (1)	12 (1)
L_{11}	55 (1) rad^2	55 (1) rad^2
L_{33}	62 (1)	63 (2)

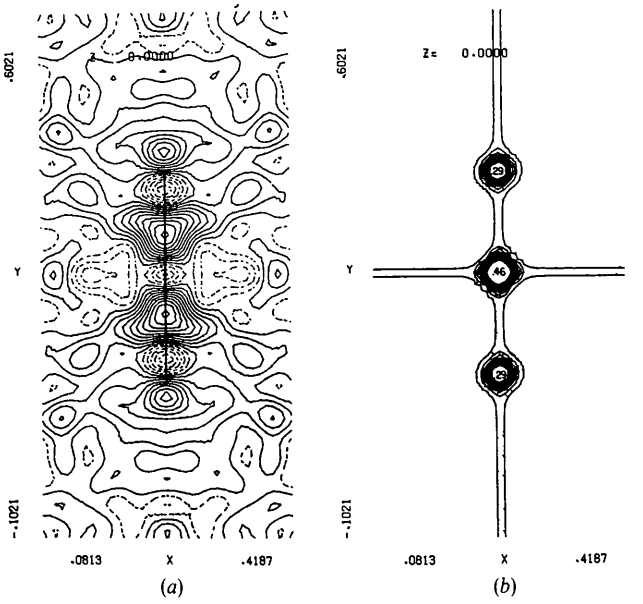

Fig. 1. Azide ion $\Delta\varrho(X-X)$ density in the (001) plane. (*a*) Experimental deformation density. Contours are at 0·05 e $Å^{-3}$ with negative contours dashed. (*b*) Error distribution. Contours at 0·015 e $Å^{-3}$, lowest contour is 0·045 e $Å^{-3}$. Highest contours omitted and labeled with maximum values.

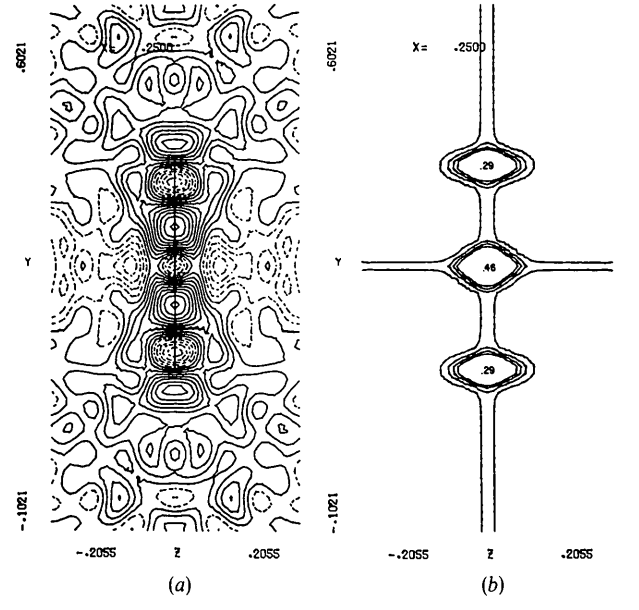

Fig. 2. Azide ion $\Delta\varrho(X-X)$ density in the (110) plane. Contours as in Fig. 1. (*a*) Experimental density. (*b*) Error distribution.

tors gives a significantly better fit to the low-order data. Despite the deficiencies of the wavefunction in the bonding region, the description of the overall charge distribution in the N_3^- ion is apparently good.

Rigid-body translational and librational thermal parameters were fit to the individual high-order nitrogen parameters by the procedure of Schomaker & Trueblood (1968). Rigid-body parameters for the azide ion are compared with neutron diffraction results in Table 3.

Deformation densities calculated from high-order X-ray parameters, $\Delta\varrho_{X-X}$, are plotted for the azide ion in Figs. 1 and 2. Included in each figure is a plot of the total estimated standard deviation in the deformation density. Peaks commonly associated with the bond and lone-pair densities are found between the nitrogens (0·46 e $Å^{-3}$) and at the end of the molecule (0·37 e $Å^{-3}$). Estimated standard deviations of the peak heights are 0·06 e $Å^{-3}$ and 0·05 e $Å^{-3}$ respectively.

Sections of $\Delta\varrho_{X-X}$ through the bond and lone-pair peaks perpendicular to the molecular axis are shown in Fig. 3. The bond peak is nearly cylindrically symmetric, but the lone-pair is elongated in the **c** direction which corresponds to the largest component of thermal libration. The largest peaks in the vicinity of K^+ are 0·10 e $Å^{-3}$.

Using a scale factor determined by refinement on k with fixed neutron parameters, large positive peaks are found for $\Delta\varrho_{X-N}$ at the nitrogen centers in the N_3^- molecule. A similar result has been found by Choi & Prince (1976) using the X-ray data of Müller (1972). The anomalous peaks in the $\Delta\varrho_{X-N}$ density are due to the large discrepancy between the X-ray and neutron thermal parameters for the K^+ ion. Since potassium dominates the X-ray scattering, a large error is introduced into the scale factor. When high-order (HF) X-ray thermal parameters for K^+ are substituted for the neutron values in the refinement of the scale factor the $\Delta\varrho_{X-N}$ density (Fig. 4) of the azide ion is very similar to the $\Delta\varrho_{X-X}$ density.

To investigate the effects of series termination error on the deformation density, $\Delta\varrho_{X-X}$ has been calculated for various values of $(\sin\theta/\lambda)_{max}$. In Fig. 5, $\Delta\varrho_{X-X}$ has

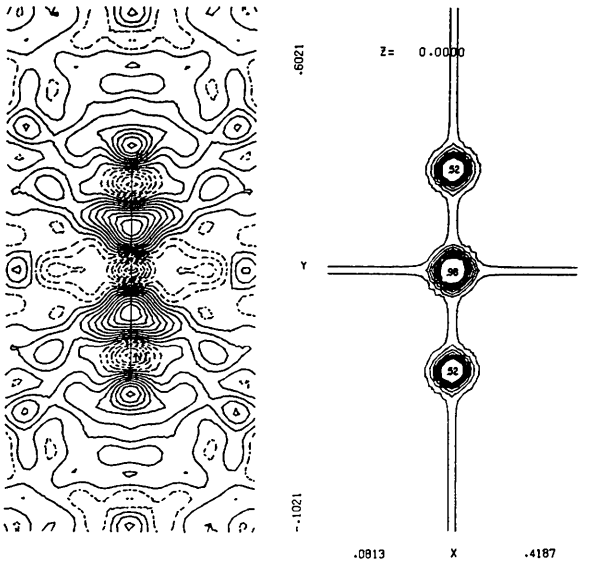

Fig. 4. Azide ion $\Delta\varrho(X-N)$ density in the (001) plane. Contours as in Fig. 1. (*a*) Experimental density. (*b*) Error distribution.

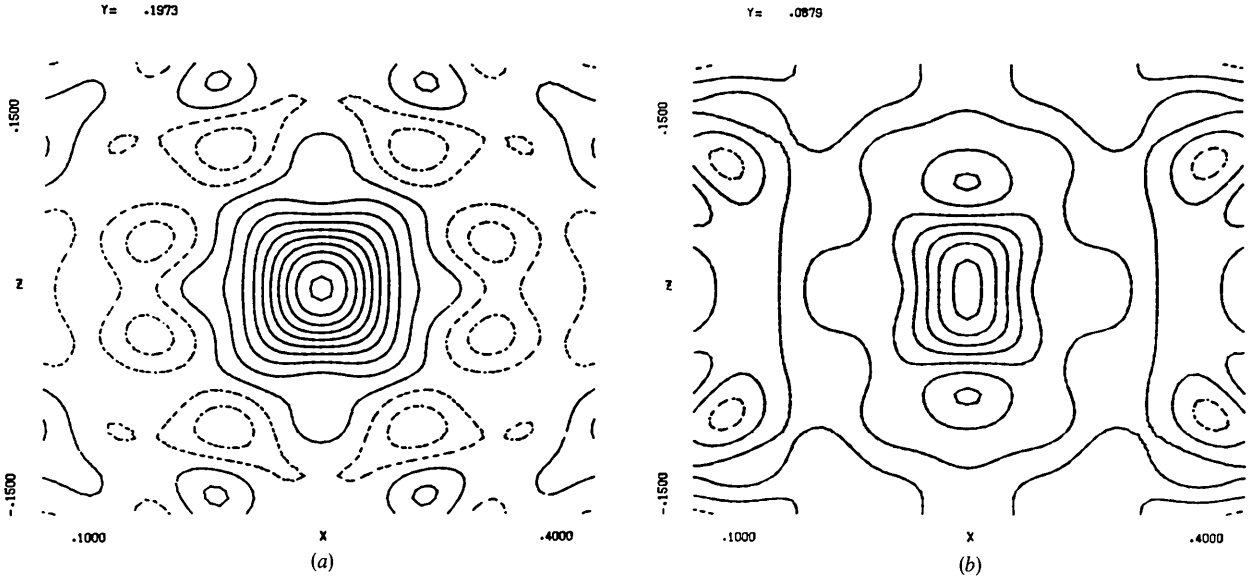

Fig. 3. Sections of $\Delta\varrho(X-X)$ perpendicular to the N_3^- molecular axis. Contours at 0·05 e $Å^{-3}$. (*a*) Section through bond peak maximum. (*b*) Section through lone-pair peak maximum.

been plotted using only the data within the Cu sphere ($\sin\theta/\lambda < 0{\cdot}64$ Å^{-1}). In contrast with Fig. 1, the deformation density at this resolution contains only the major features but little of the fine detail in the shape of the peaks.

A measurement of the deformation density at a particular temperature may be considered quantative if it has converged to the value at infinite resolution. In Fig. 6, the bond and lone-pair peak heights are plotted as a function of the resolution limit $(\sin\theta/\lambda)_{max}$. Even at room temperature, it is evident that data with $(\sin\theta/\lambda)_{max}$ at least 1·00 Å^{-1} must be included to give quantitative information on the lone-pair density. While low-temperature studies will give more detailed information on bonding, even higher order data will be required to give quantitative results (Coppens & Lehmann, 1976).

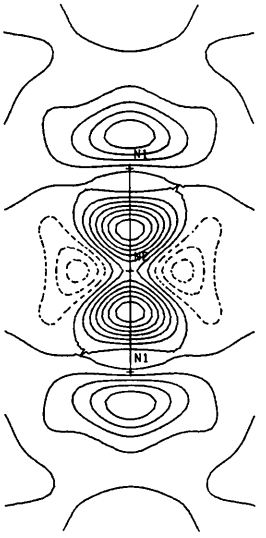

Fig. 5. Azide ion $\Delta\varrho(X-X)$ density as in Fig. 1, but including only X-ray measurements for $\sin\theta/\lambda < 0{\cdot}64$ Å^{-1}.

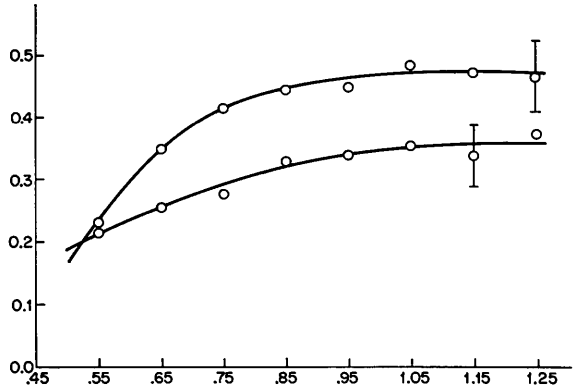

Fig. 6. Bond and lone-pair peak heights plotted as a function of $(\sin\theta/\lambda)_{max}$. Upper curve is the bond peak and the lower curve the lone-pair peak.

Support of this work by the National Science Foundation is gratefully acknowledged. The author is indebted to Professor P. Coppens for many helpful discussions.

References

BECKER, P. J. & COPPENS, P. (1975). *Acta Cryst.* A**31**, 417–425.

BLESSING, R. H., COPPENS, P. & BECKER, P. (1974). *J. Appl. Cryst.* **7**, 488–492.

CHOI, C. S. & PRINCE, E. (1976). *J. Chem. Phys.* **64**, 4510–4516.

COPPENS, P. (1975). *MTP International Review of Science, Physical Chemistry Series, Chemical Crystallography*. Vol. 11, pp. 21–56. London: Butterworths.

COPPENS, P. & LEHMANN, M. S. (1976). *Acta Cryst.* B**32**, 1777–1784.

COPPENS, P., LEISEROWITZ, L. & RABINOVICH, D. (1965). *Acta Cryst.* **18**, 1035–1038.

COPPENS, P. & STEVENS, E. D. (1976). *Advances in Quantum Chemistry*, Vol. 10. New York: Academic Press.

CROMER, D. T. & LIBERMAN, P. (1970). *J. Chem. Phys.* **53**, 1891–1898.

DOYLE, P. A. & TURNER, P. S. (1968). *Acta Cryst.* A**24**, 390–397.

MÜLLER, U. (1972). *Z. anorg. Allgem. Chem.* **392**, 159–166.

REES, B. (1976). *Acta Cryst.* A**32**, 483–488.

SCHOMAKER, V. & TRUEBLOOD, K. N. (1968). *Acta Cryst.* B**24**, 63–76.

STEVENS, E. D. (1973). *Experimental Determination of Electron Density Distributions by X-ray Diffraction*. Thesis, Univ. of California, Davis.

STEVENS, E. D. & COPPENS, P. (1976). *Acta Cryst.* A**32**, 915–917.

STEVENS, E. D. & HOPE, H. (1975). *Acta Cryst.* A**31**, 494–498.

STEVENS, E. D. & HOPE, H. (1977). *Acta Cryst.* Submitted for publication.

STEVENS, E. D., RYS, J. & COPPENS, P. (1977*a*). *J. Amer. Chem. Soc.* **99**, 265–267.

STEVENS, E. D., RYS, J. & COPPENS, P. (1977*b*). In preparation.